JOURNAL OF SOLID STATE CHEMISTRY **133,** 302–309 (1997)
ARTICLE NO. SC977491

A Unified Picture for Icosahedral Cluster Solids in Boron-Based and Aluminum-Based Compounds

K. Kimura, M. Takeda, M. Fujimori, R. Tamura, and H. Matsuda

Department of Materials Science, University of Tokyo, Tokyo 113, Japan

and

R. Schmechel and H. Werheit

Solid State Physics Laboratory, Gerhard Mercator University of Duisburg, D-47048 Duisburg, Germany

Received May 19, 1997; accepted May 27, 1997

Discussions are presented to get a unified picture for the boron-based and aluminum-based compounds constructed from icosahedral clusters. Twelve-atom centerless icosahedra, Al_{12} and B_{12}, have a covalent bonding nature, though 13-atom centered ones, Al_{13} and B_{13}, are metallic. Stabilization mechanisms for the both compounds, the Hume–Rothery mechanism and the Jahn–Teller effect, are closely related. There are vacant sites in the second shell of the multi-shell structure for boron compounds. When these sites are occupied by dopant metal atoms, the cluster structure, dc conductivity, and optical conductivity of the boron compounds approach those of the aluminum compounds. Photoconduction is observed in aluminum compounds as well as in boron compounds. Photocurrent arising from carrier excitation through the localized states in the pseudogap and the intrinsic acceptor levels are important for aluminum and boron compounds, respectively. © 1997 Academic Press

INTRODUCTION

Both aluminum and boron belong to the third group of the periodic table and have some solid state structures that are constructed of icosahedral clusters. In aluminum-based systems, we know several kinds of icosahedral quasicrystal and approximant, and in boron-based systems, icosahedral boron-rich solids are known (1, 2). Figure 1 shows the conductivity at 0 K and the periodic length of the crystalline structure for some aluminum- and boron-based systems. The conductivity at 0 K is finite for metals and zero for semiconductors. The periodic length is finite for crystalline approximants and infinite for quasicrystals. The aluminum-based icosahedral compounds, which can produce the quasicrystalline structure and are originally metallic, approach a semiconductor; i.e., the electrical conductivity at 0 K decreases to 0 with increasing structural order (3, 4). The boron-based compounds, which produce the crystalline structure and are semiconducting, approach a quasicrystal; i.e., the unit cell size increases when the composition is turned (5).

In this paper, some discussions are presented to get the unified picture for the above two groups of materials constructed of the icosahedral cluster.

CLUSTER STRUCTURE

Both of the compounds have the multiple-shell structure of clusters with icosahedral symmetry. Figure 2 compares the multiple-shell structures in the aluminum- and boron-based systems. For aluminum-based systems, there are two types of icosahedral alloys, the Frank–Kasper (FK) type and the Mackay–Icosahedral (MI) type. As for the Al–Li–Cu FK phase (the 1/1 cubic approximant phase) (6), the first shell is an icosahedron, the second is a triacontahedron, which is constructed of a dodecahedron and an icosahedron, and the third is a truncated triacontahedron (a soccer ball cluster). In the case of the Al–Mn–Si MI-type 1/1 cubic approximant (7), the second shell is constructed of an icosahedron and a truncated icosahedron instead of an dodecahedron and the third shell is absent. In both approximant structures, each multiple-shell cluster is located at a vertex and a body centered site. The structures of both types of quasicrystals are considered to be constructed of their respective multiple-shell clusters.

In the β-rhombohedral boron structure, a B_{84} cluster is located at each vertex of the rhombohedral unit cell (8). The cluster is constructed by connecting 12 B_6 half icosahedra to the center B_{12} along the fivefold axes. This structure is considered to be the 0/1–2/0 rhombohedral approximant. For the B_{84} cluster, as shown in Fig. 5, the first shell is an

0022-4596/97 $25.00

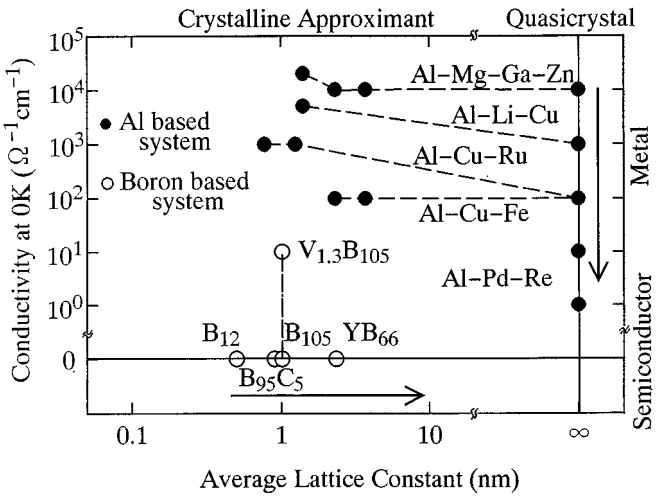

FIG. 1. DC conductivity at 0 K and periodic length of structure for some icosahedral aluminum-based and boron-based systems.

icosahedron, the second is an icosahedron, and the third is a soccer ball cluster.

Commonly in both compounds, the first shell is the icosahedron and the third shell is the soccer ball cluster (this is missing in the MI type). Although the second shell is constructed of the icosahedron and the dodecahedron (FK type) or the truncated-icosahedron (MI type) in the aluminum compounds, the latter is missing in the boron compounds. The atom density in the second shell in the boron compounds is low, and it is considered that there are vacant sites in the second shell. A part of the dodecahedral vacant sites are known as the doping sites described in the Electronic Transport Section.

The fact mentioned above is the origin of difference in coordination number for both compounds. In aluminum-based systems, the coordination number of most atoms is 11 or 12 like usual metallic systems. In boron-based systems, it is usually 6, which is smaller than that of metallic systems but is larger than 2, 3, or 4, that of usual covalent bonding systems.

ELECTRONIC STATES OF ICOSAHEDRAL CLUSTER

There are two types of icosahedral clusters, 13 atoms (with the center atom) and 12 atoms (without the center atom) clusters. The packing fraction of the 13-atom icosahedron is 0.727, which is smaller than 0.756, that of the 13-atom close-packed structure, but is greater than 0.680, that of body-centered cubic structure. The 13-atom icosahedron must be stable under metallic bonding and may be called to be a metallic cluster. On the other hand, the packing fraction of the 12-atom icosahedron is 0.520, which is much smaller than those of metallic clusters and approaches 0.340, that of the diamond structure. The 12-atom icosahedron cannot be stable under metallic bonding.

The 12-atom icosahedron is one or only one solution to produce covalent bonding structure for the third group elements with three valence electrons. Typical covalent bonds in semiconductors are sp^3 for the fourth group elements Si, Ge, and Sn, sp^2 for the fourth group element C, p^3 for the fifth group element P, and p^2 for the sixth group elements Se and Te. These bonds are two-centered ones, in which each of two atoms provides one electron and they share two electrons. When an atom produce one bond, the number of its owned electrons increases by one. The fourth, fifth, and sixth group elements can apparently construct the closed shell of s and p orbitals by producing four, three, and two bonds, respectively. However, the third group elements cannot construct the closed shell in the same way. Since they are electron deficient to complete the covalent bonding, they must construct the multi-centered covalent bonds to save electrons. For example, in the simple three centered bond, each of three atoms provides two thirds electron and they share two electrons. This bonding is realized in the inter-icosahedral bonds in the α-rhombohedral boron (9). The intra-icosahedral bonding of the 12-boron-atom icosahedron (B_{12}) is considered to be multi-centered. Each atom of B_{12} has one outer bond, which is usually a two-centered bond, along the fivefold axis. Each atom provides one electron to this outer bond and two electrons to the intra-icosahedral bonds. The number of electrons distributed to each triangle of B_{12} is $2 \times 12/20 = 1.2$. Since each atom has one outer bond and five neighbors of the triangle, it shares $2 + 1.2 \times 5 = 8$ electrons and can produce a closed shell. This calculation is too simple and the real situation is more complicated; i.e., the B_{12} is still two electrons deficient as mentioned in the next section.

Electronic states of the 12-atom icosahedron of boron and aluminum were calculated using the *ab initio* molecular orbital method (10). The B_{12} cluster is the most stable at a B–B distance of 0.175 nm, which is consistent with the experimental value, and can be stable at a distance shorter than 0.2 nm. The Al_{12} cluster can be stable at a Al–Al distance shorter than 0.255 nm, which is similar to those in the icosahedral aluminum compounds, and shorter than 0.28 nm, that in fcc Al structure. Under the condition of the shorter atom–atom distance, the electronic states of the B_{12} and Al_{12} icosahedral clusters are exactly the same.

Table 1 shows the stable position outside of the icosahedral clusters of aluminum and boron for some elements. They are the results of structural optimization using the MOPAC program (11). Three positions described by v, ec, and f are shown in Fig. 3. As for the 13-atom icosahedron, Al_{13} or B_{13}, all three elements are stabilized at the position of f, which is the stable one for the rigid sphere packing. On the other hand, for the 12-atom clusters, Al_{12} or B_{12}, H and Li are stabilized at the position of v and terminate the dangling bond of B_{12}, and Al or B is stabilized at the position of ec and looks like constructing the three-centered bond with

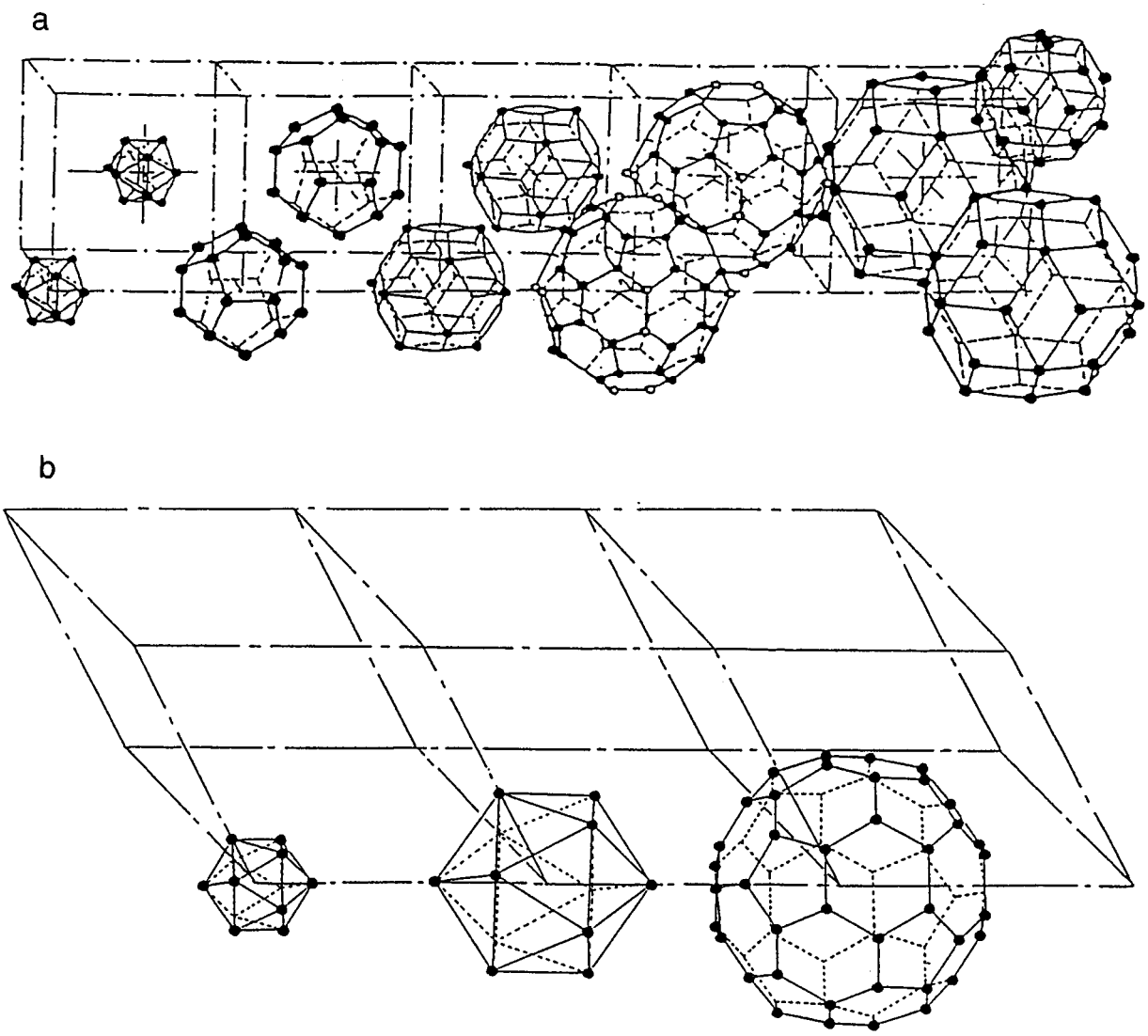

FIG. 2. Multiple shell structures in aluminum-based and boron-based systems. (a) Al–Li–Cu Frank–Kasper phase, (b) β-rhombohedral boron.

two atoms in the Al_{12} or B_{12}. These situations show also that Al_{13} and B_{13} are metallic and Al_{12} and B_{12} have a covalent bonding nature.

TABLE 1
The Stable Position outside of the Icosahedral Clusters of Aluminum and Boron for Some Elements

	Elements (X)		
Clusters	H	Li	Al or B
$Al_{12} + X$ $B_{12} + X$	v	v	ec
$Al_{13} + X$ $B_{13} + X$	f	f	f

These situations show that Al_{12} with Al–Al distances shorter than 0.255 nm has covalent bonding nature. It is interesting to mention that electronic transport properties (12) are rather metallic in Mg–Al–Zn quasicrystals constructed of Al_{13}, and are far from that of usual metals in Al–Li–Cu and MI-type quasicrystals constructed of Al_{12}.

ELECTRONIC TRANSPORT

Figure 4a shows the temperature dependence of dc conductivity, σ, for some aluminum-based icosahedral quasicrystals (12, 13). Electrical conductivity of the quasicrystal is extremely low as compared with usual metals because of the pseudogap and the localization tendency of electrons near the Fermi level (12). Up to now all discussions concerning an interpretation of the conduction mechanism of quasi-

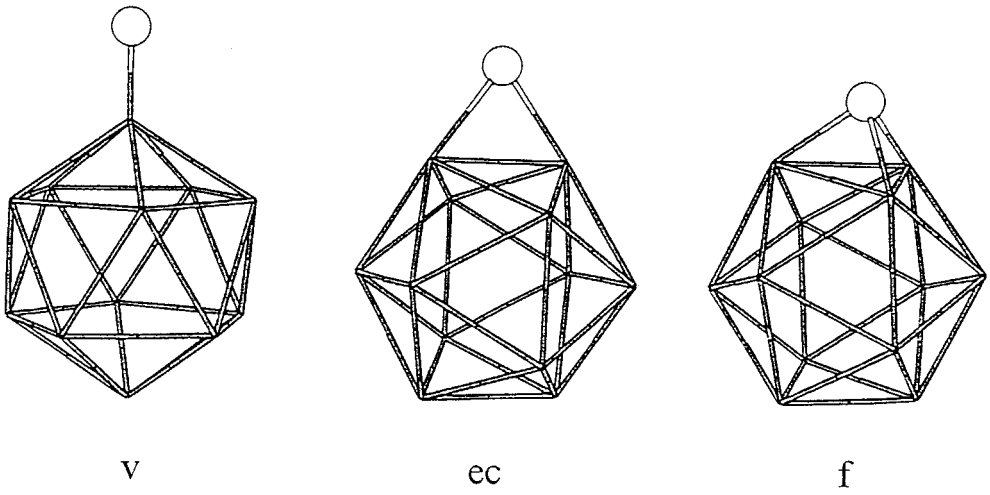

FIG. 3. Three stable atom positions outside of icosahedral clusters of boron.

crystals seem to be clarified mainly into two pictures (13). In one of them, it is considered that temperature variation of the carrier density, n, plays an essential role in that of conductivity, $\sigma = ne\mu$. In the other, it is assumed that the temperature dependence of the mobility, μ, is responsible for that of σ. The band structure effect, which is based on a spiky band and a narrow gap in the density of states both with the width of about 10 meV, plays a significant role in the former. In the latter, localization effects such as the weak-localization effect are considered to explain electronic transport of quasicrystals and even hopping conduction of electrons in rather strongly localized states has been proposed by several authors. The value of σ of the quasicrystals is comparable with that of a doped semiconductor as shown in Fig. 4, and the above two pictures for the conduction mechanism are not metallic but semiconductor-like already.

Figure 4b shows the temperature dependence of dc conductivity for Li- and some transition metal-doped β-rhombohedral boron crystals (B_{105}) (14, 15). It shows that σ increases by several orders of magnitude after metal doping of several at.% and has the variable range hopping (VRH) type behavior. Although such a non-activated conductivity may also be explained by the freezing out of multi-phonon hopping processes (16), there is no suitable formalism for this mechanism. As the following discussions do not depend on the mechanism for the temperature dependence of conductivity, they are treated with a VRH formalism in this paper. According to Mott's law of VRH conduction (17), σ is expressed as

$$\sigma = \sigma_0 \exp[-(T_0/T)^{1/4}], \quad T_0 = 60\alpha^3/\pi N(E_F)k_F, \quad [1]$$

where α^{-1} is the localization length of the wave function of the carrier and $N(E_F)$ is the density of states at the Fermi energy. Figure 5 shows the metal concentration, x, dependence of T_0^{-1}. In the case of usual doping, e.g., an impurity element in silicon or an alkali metal in C_{60}, T_0^{-1} increases monotonically with increasing dopant concentration. First, $N(E_F)$ increases; then α^{-1} increases near the metal–insulator transition, and it becomes infinite at the transition. As shown in Fig. 4, in the case of Li, Cu, and Ni, unusually, T_0^{-1} increases, reaches the maximum, and decreases with further increasing x.

This unusual behavior can be explained as follows (14, 15). Since the B_{12} is two electrons deficient, one of the highest fourfold-degenerated intra-icosahedral orbitals is empty and separate from the occupied ones by the distortion of the B_{12}. It is thought that this unoccupied orbital leads to an intrinsic acceptor band above the valence band edge in the β-rhombohedral boron (18). Doped electrons from metal atoms occupy this band and show VRH conduction between localized states of the band. In this case, when number of electrons in this band exceeds half of all states in it, T_0^{-1} may change from increase to decrease with increasing x. Since the maximum values of T_0^{-1} in Fig. 5 depend on the kind of dopant metals, the rigid band model cannot be applicable. This situation can be explained by considering the hybridization of the impurity levels of the dopant metals and the intrinsic acceptor band of β-rhombohedral boron. Table 2 and Fig. 6 show the doping sites and their occupancy for each metal atom in the rhombohedral unit cell of β-rhombohedral boron. The structure of the unit cell can be viewed in two ways as shown in Fig. 6a and 6b. As shown in 6a, the A_1 hole is the nearest to B_{12} and has four neighbors of them; thus, the level of the metal occupying the A_1 hole must be hybridized with the intrinsic acceptor level of B_{12}. It is found that the greater the occupancy of the A_1 hole in Table 2, the greater the maximum value of T_0^{-1} in Fig. 5.

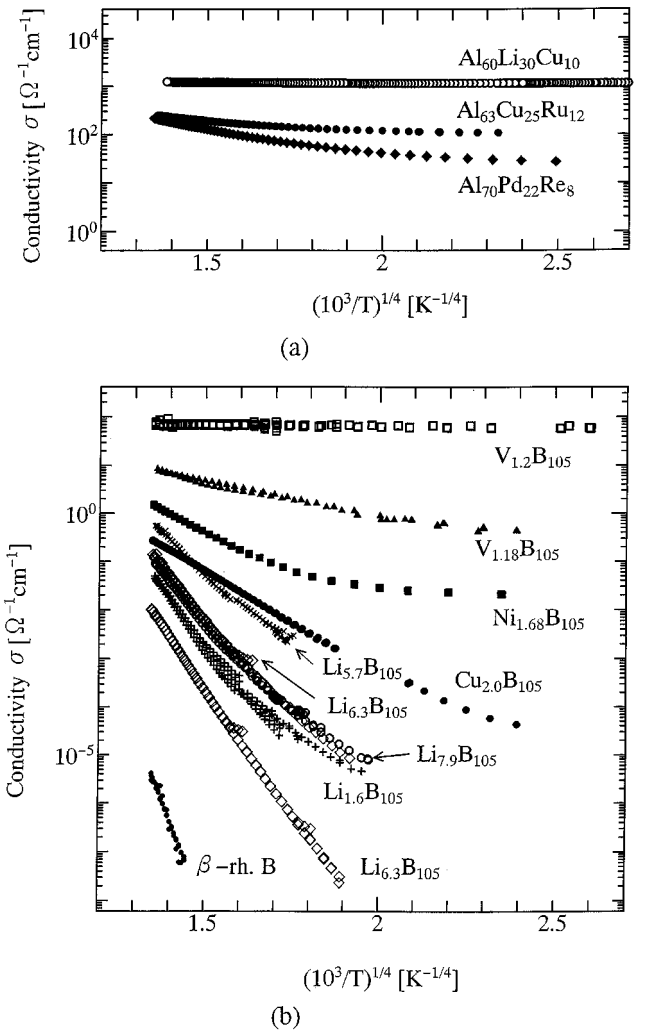

FIG. 4. Temperature dependence of dc conductivity for some (a) icosahedral aluminum-based quasicrystals and (b) metal-doped β-rhombohedral boron crystals.

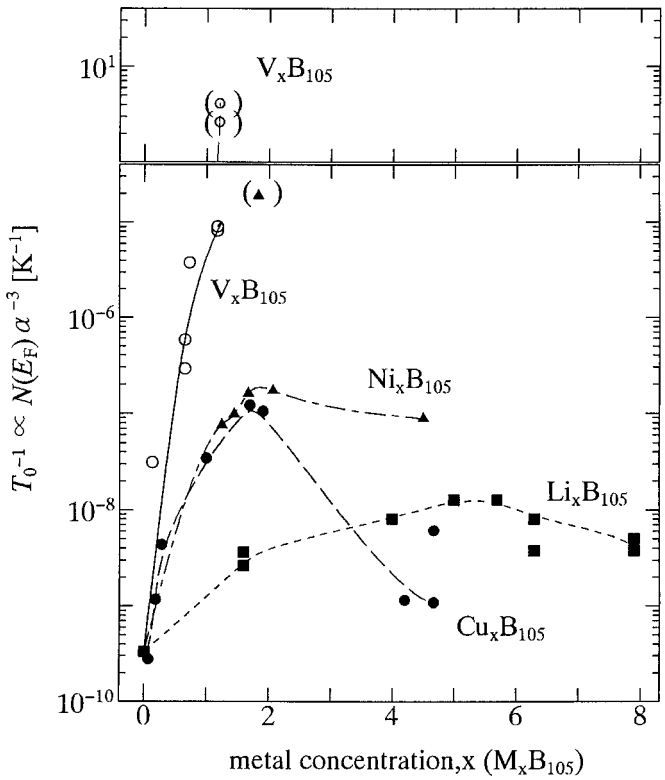

FIG. 5. Metal concentration dependence of T_0^{-1} of the variable range hopping formula for some metal-doped β-rhombohedral boron crystals.

As for V doping, the metal–insulator transition may occur at the highest concentration. The value of conductivity and its temperature dependence of the highest V concentration sample ($V_{1.2}B_{105}$) are similar to those of the lowest conductive quasicrystals ($Al_{70}Pd_{22}Re_8$ and $Al_{63}Cu_{25}Ru_{12}$), as shown in Fig. 4.

In Fig. 7a and 7b, the spectra of the optical conductivity of some boron-rich structures is compared with the according spectra of the Al–Pd-Re quasicrystals measured with the same equipment (19), and additionally for comparison with the spectra of Al–Cu–Fe (20) and Al–Mn–Pd (21) reported from literature. Characteristic features of optical conductivity in the aluminum-based quasicrystals have been considered to be a very small Drude contribution, which is not apparent in the spectra as shown in Fig. 7b, and a large contribution of interband transition across the pseudogap (20, 21). Although the spectra of the Al–Pd–Re quasicrystals in Fig. 7b has the same features, the value of conductivity is one order smaller than those of the others and than even those reported previously for the same alloy system (22). The optical conductivity of the same Al–Pd–Re sample in Fig. 6b was determined by spectroscopic ellipsometry in the 2.5–7.5 eV range (23), which has no ambiguity of the Kramers–Kronig transformation. The value at the lowest energy, which corresponds to 20,000 cm^{-1}, is consistent with that in Fig. 7b. Therefore, the origin of discrepancy between the conductivity values in Fig. 7b and those

TABLE 2
Occupancy of Doping Sites in Metal-Doped β-Rhombohedral Boron

Composition	Doping site occupancy (%)		
	A_1 hole (2 sites/unit cell)	E hole (2 sites/unit cell)	D hole (6 sites/unit cell)
$Li_{7.9}B_{105}$	0.0	100.0	100.0
$Cu_{4.2}B_{105}$	7.9	33.4	59.9
$Ni_{2.16}B_{105}$	44.7	0.0	21.6
$V_{1.62}B_{105}$	64.0	0.0	5.3

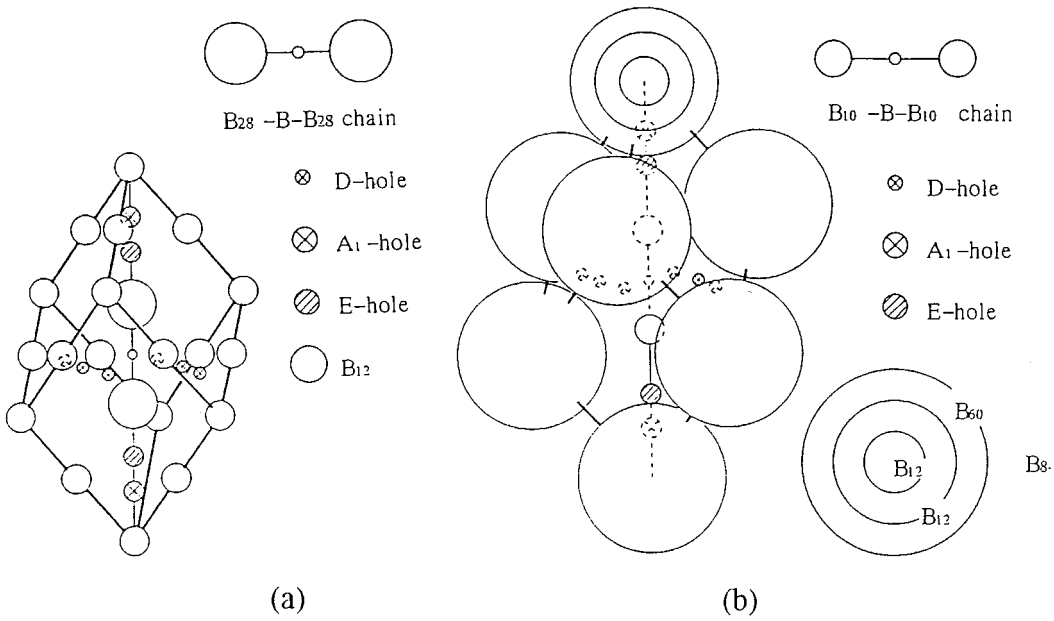

FIG. 6. Crystalline structure of β-rhombohedral boron shown in two different ways, (a) and (b).

reported previously in the same Al–Pd–Re system is considered to be the ambiguity of the large sample dependence of physical properties in this alloy systems. The spectra of the optical conductivity of V-doped β-rhombohedral boron in Fig. 7a have similar values and the same features as those of Al–Pd–Re quasicrystals in Fig. 7b.

It is interesting to mention that, as shown in Fig. 6b, the A_1 hole is a part of the dodecahedral vacant sites in Fig. 2, which are missing in the second shell in the boron compounds compared to the FK-type aluminum compounds. Therefore, when the multiple-shell cluster structure of the boron compound (β-rhombohedral boron) approaches that

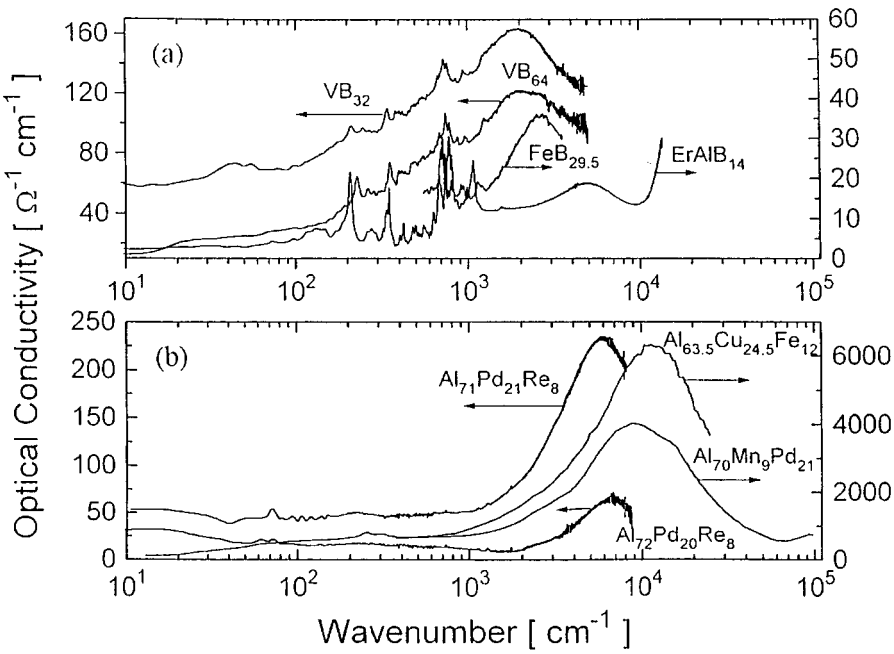

FIG. 7. Optical conductivity spectra for some (a) metal-doped β-rhombohedral boron crystals and (b) icosahedral aluminum-based quasicrystals.

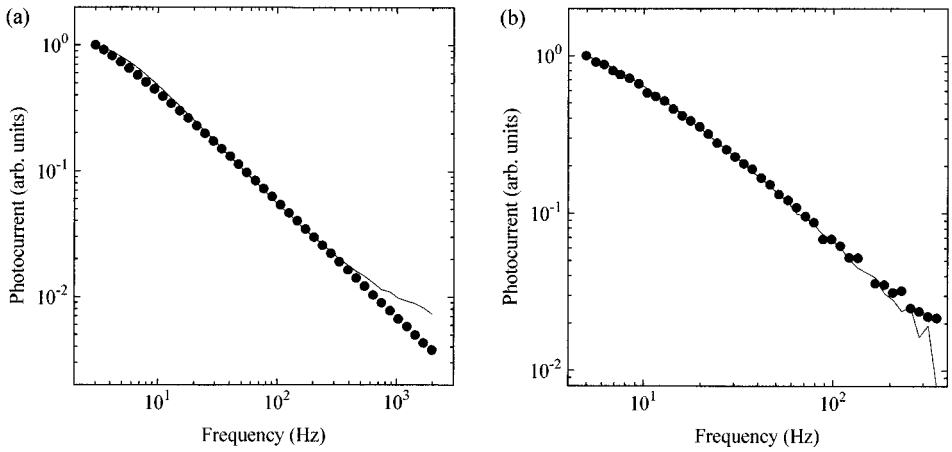

FIG. 8. Frequency dependence of photocurrent for (a) β-boron and (b) $Al_{70.5}$–Pd_{21}–$Re_{8.5}$. Solid lines are calculated from phase shift data.

of the aluminum compounds (especially FK-type Al–Li–Cu) by doping to the A_1 hole, not only the behavior of dc conductivity but also that of optical conductivity of the former seem to approach those of the latter.

PHOTOCONDUCTIVITY

Photoconductivity is widely used to investigate photocarrier generation process, localized states in a band gap, and transport properties in semiconductor. We apply this technique to both the boron system and the aluminum system. The modulated photocurrent method is a very sensitive measurement. An intensity-modulated monochromatic light is illuminated on a sample between two electrodes, and the consequent photocurrent (the magnitude and the phase shift between the excitation light and the photocurrent) is measured with a lock-in amplifier. For a conventional semiconductor, the profile of localized states can be estimated by analyzing the frequency dependence of the phase shift on the basis of a simple model which assumes band-to-band excitation, unipolar photocurrent, and trap-limited conduction in extended states (24).

Figure 8a shows the frequency dependence of the photocurrent for β-rhombohedral boron (solid circles). The data were analyzed by the above model. The photocurrent was calculated from the phase shift data and we found that it is inconsistent with that observed. As a consequence, the photoconduction process in β-rhombohedral boron is not as simple as assumed in the model, and it is considered that the intrinsic acceptor level plays an important role in the process. An analysis taking account of the acceptor level (solid line in Fig. 8a) can explain the observed photocurrent very well (24).

As shown in Fig. 8b, we succeeded in measuring the photocurrent in Al–Pd–Re quasicrystal for the first time. The fact that the photocurrent is observed in quasicrystal is direct evidence for the existence of the pseudogap. The same analysis as done for β-rhombohedral boron was carried out, and we also found an consistency between observed (solid circles) and calculated (solid line) photocurrent. Such a situation, i.e., localized states are important not only for trapping carriers but also for photogeneration of carriers, is a common feature for both systems (25).

CONCLUSION

The 12-atom icosahedra, Al_{12} and B_{12}, have the same molecular orbitals, i.e., covalent bonding electronic structures, though the 13-atom icosahedra, Al_{13} and B_{13}, are metallic. Both the aluminum- and boron-based compounds have the multiple-shell structure of clusters with the icosahedral symmetry. There are dodecahedral vacant sites in the second shell of the boron one. When a metal atom occupies a part of the dodecahedral vacant sites in β-rhombohedral boron, hybridization between a level of the metal atom and the intrinsic acceptor level occurs, and the electronic properties of the β-boron approach the metal–insulator transition. By this doping, the cluster structures, the behavior of dc conductivity, and the optical conductivity spectra for the β-boron approach those of the aluminum compounds. Photocurrent was observed in Al–Pd–Re quasicrystal, and this result supports the existence of the pseudogap.

REFERENCES

1. D. Emin, T. L. Aselage, A. C. Switendick, B. Morosin, and C. L. Beckel (Eds.), "Boron-Rich Solids," AIP Conf. Proc. 231. Am. Inst. of Physics, New York, 1991.
2. R. Uno, and I. Higashi (Eds.), "Proc. 11th Int. Symp. Boron, Borides and Related Compounds," *JJAP Series* 10. JJAP, Tokyo, 1994.

3. Y. Honda, K. Edagawa, A. Yoshioka, T. Hashimoto, and S. Takeuchi, *Jpn. J. Appl. Phys.* **33,** 4929 (1994).
4. F. S. Pierce, Q. Guo, and S. J. Poon, *Phys. Rev. Lett.* **73,** 2220 (1994).
5. M. Takeda, K. Kimura, A. Hori, H. Yamashita, and H. Ino, *Phys. Rev.* B **48,** 13159 (1993).
6. M. Audier and P. Guyot, *in* "Quasicrystalline Materials" (C. Janot and J. M. Dubois, Eds.), p. 181. World Scientific, Singapore, 1988.
7. I. Higashi, *in* "Boron-Rich Solids" (D. Emin, T. Aselage, C. L. Beckel, I. A. Howard and C. Wood , Eds.), AIP Conf. Proc. 140, p. 1. Am. Inst of Physics, New York, 1986.
8. R. Naslain, *in* "Boron and Refractory Borides" (V. I. Matkonich, Ed.), p. 139. Springer-Verlag, New York, 1977.
9. D. Emin, *Phys. Today* (*Jan.* 55 1987).
10. T. Hatakeyama and H. Kamimura, *in* "Proc. 20th. Int. Conf. Physics of Semiconductors" (E. M. Anastassakis, Ed.), p. 730. World Scientific, Singapore, 1990.
11. M. Fujimori and K. Kimura, *J. Solid State Chem.* **133,** 310 (1997).
12. K. Kimura and S. Takeuchi, *in* "Quasicrystals: The State of the Art" (D. P. DiVincenzo and P. J. Steinhardt, Eds.), p. 313. World Scientific, Singapore, 1991.
13. R. Tamura, K. Kirihara, K. Kimura, and H. Ino, *in* "Proc. 5th. Int. Conf. Quasicrystals" (C. Janot and R. Mosseri, Eds.), p. 539. World Scientific, Singapore, 1995.
14. H. Matsuda, T. Nakayama, K. Kimura, Y. Murakami, H. Suematsu, M. Kobayashi, and I. Higashi, *Phys. Rev. B* **52,** 6102 (1995).
15. H. Matsuda, T. Nakayama, N. Tanaka, K. Kimura, H. Suematsu, Y. Murakami, M. Kobayashi, and I. Higashi, *J. Phys. Chem. Solids* **57,** 1167 (1996).
16. D. Emin, *Phys. Rev. Lett.* **32,** 303 (1974).
17. N. F. Mott and E. A. Davis, "Electronic Processes in Non-Crystalline Materials." Clarendon Press, Oxford, 1979.
18. R. Franz and H. Werheit, *in* "Boron-Rich Solids" (D. Emin, T. L. Aselage, A. C. Switendick, B. Morosin, and C. L. Beckel, Eds.), AIP Conf. Proc. 231, p. 29. Am. Inst. of Physics, New York, 1991.
19. H. Werheit, R. Schmechel, K. Kimura, R. Tamura, and T. Lundstrom, *Solid State Commun.* **97,** 103 (1995).
20. C. C. Homes, T. Timusk, X. Wu, Z. Altounian, A. Sahnoune, and J. O. Strom-Olsen, *Phys. Rev. Lett.* **67,** 2694 (1991).
21. L. Degiorgi, M. A. Chernikov, C. Beeli, and H. R. Ott, *Solid State Commun.* **87,** 721 (1993).
22. D. N. Basov, F. S. Pierce, P. Volkov, S. J. Poon, and T. Timusk, *Phys. Rev. Lett.* **73,** 1865 (1994).
23. C. Janowitz and K. Kimura, unpublished.
24. H. Oheda, *J. Appl. Phys.* **52,** 6693 (1981).
25. M. Takeda, R. Tamura, Y. Sakairi, and K. Kimura, *J. Solid State Chem.* **133,** 224 (1997).